Color Switching Hot Paper

DOI: 10.1002/anie.201410408

Enhanced Photoreversible Color Switching of Redox Dyes Catalyzed by Barium-Doped TiO_2 Nanocrystals**

*Wenshou Wang, Yifan Ye, Ji Feng, Miaofang Chi, Jinghua Guo, and Yadong Yin**

Abstract: *Colloidal barium-doped TiO_2 nanocrystals have been developed that enable the highly reversible light-responsive color switching of redox dyes with excellent cycling performance and high switching rates. Oxygen vacancies resulting from the Ba doping serve as effective sacrificial electron donors (SEDs) to scavenge the holes photogenerated in TiO_2 nanocrystals under UV irradiation and subsequently promote the reduction of methylene blue to its colorless leuco form. Effective color switching can therefore be realized without relying on external SEDs, thus greatly increasing the number of switching cycles. Ba doping can also accelerate the recoloration under visible-light irradiation by shifting the absorption edge of TiO_2 nanocrystals to a shorter wavelength. Such a system can be further casted into a solid film to produce a rewritable paper on which letters and patters can be repeatedly printed using UV light and then erased by heating; this process can be repeated for many cycles and does not require additional inks.*

Photoreversible color-switching materials have attracted increasing attention owing to their promising applications in a wide variety of fields, such as optical displays, data storage, optoelectronic devices, and sensors.[1] Significant efforts have previously been made to develop various chromophores that are capable of photoisomerization, which however still face challenges in practical applications owing to limitations in reversibility and switching rates.[2] Recently we have described a new photoreversible color-switching system that integrates the photocatalytic activity of TiO_2 nanocrystals and the redox-driven color-switching properties of organic dye molecules, such as methylene blue (MB).[3] A key component of this color-switching system was the nonionic polymer poly[(ethylene glycol)-*b*-(propylene glycol)-*b*-(ethylene glycol)] (P123), which binds to the TiO_2 nanocrystal surface and acts as an effective sacrificial electron donor (SED) to scavenge photogenerated holes. Upon UV irradiation, the photogenerated holes by TiO_2 nanocrystals are captured by surface-bound SED molecules, and the surviving photogenerated electrons reduce blue MB to colorless LMB. Visible-light irradiation can dramatically enhance the recoloration rate by photocatalytic initiation of the LMB to MB transition followed by a visible-light-driven self-catalyzed LMB oxidation. By effectively stabilizing the LMB and prolonging the colorless state, the system can be cast into a solid film and used as an imaging layer in the fabrication of rewritable paper that can be printed and erased repeatedly.[4] Although TiO_2 has an excellent chemical stability, the color switching of the TiO_2/MB solution can typically only be cycled approximately ten times because surface-bound P123 is gradually consumed during the reactions and eventually exhausted.[3] Adding free P123 to the solution could not effectively increase the number of cycles. It is therefore highly desirable to explore new mechanisms to replace P123 as the scavenger of photogenerated holes to realize significantly extended life times.

Herein, we propose to utilize oxygen vacancies in TiO_2 nanocrystals as internal SEDs to significantly improve the performance of photoreversible color switching. As one of the most important defects in metal oxides, oxygen vacancies carry unpaired electrons that could form donor levels in the electronic structure of TiO_2.[5] Whereas many methods have been reported for creating oxygen vacancies in TiO_2, doping with metal ions of valences lower than that of the parent cations (Ti) represents a convenient method for producing oxygen vacancies in the TiO_2 lattice.[6] In this work, we report that colloidal barium-doped TiO_2 nanocrystals can act as effective SEDs to capture photogenerated holes and enable highly reversible light-responsive color switching at enhanced rates. The oxygen vacancies resulting from the Ba doping are responsible for efficiently scavenging the holes photogenerated under UV irradiation. As color switching can now be enabled without relying on external SEDs, the cycling

[*] W. Wang,[+] J. Feng, Y. Yin
Department of Chemistry, University of California
Riverside, CA 92521 (USA)
E-mail: yadong.yin@ucr.edu
Y. Ye,[+]
National Synchrotron Radiation Laboratory
University of Science and Technology of China
Hefei 230029 (China)
Y. Ye[+] J. Guo
Advanced Light Source, Lawrence Berkeley National Laboratory
Berkeley, CA 94720 (USA)
M. Chi
Materials Science Division, Oak Ridge National Laboratory
Oak Ridge, TN 37830 (USA)
[+] These authors contributed equally to this work.

[**] We are grateful for financial support from the U.S. Department of Energy (DE-FG02-09ER16096). The XPS facility was acquired with funds from the U.S. National Science Foundation under the Major Research Instrumentation Program (DMR-0958796). The work performed on BL 8.0.1 and 10.3.2 at the Advanced Light Source was supported by the Director, Office of Science, Office of Basic Energy Sciences of the U.S. Department of Energy (DE-AC02-05CH11231). Y. Ye gratefully acknowledges the supervision of Dr. Junfa Zhu at the University of Science and Technology of China, and financial support from the National Basic Research Program of China (2013CB834605) and the National Natural Science Foundation of China (U1232102). We would also like to thank Dr. Josep Roque-Rosell for assistance with XAS measurements.

Supporting information for this article is available on the WWW under http://dx.doi.org/10.1002/anie.201410408.

performance can be greatly enhanced to more than 45 cycles. An additional advantage of the new system is that doping with alkali metal ions can induce a decrease in the absorption wavelength of TiO_2 nanocrystals, which can effectively repress the partial reduction of MB to LMB under visible-light irradiation, leading to a higher recoloration rate (2.5 min) than for the previous, undoped system (15 min). The excellent cycling performance and rapid switching rate render the new color-switching systems promising candidates for many technological applications, especially as rewritable media.

Ba-doped TiO_2 colloidal nanocrystals were synthesized by heating a mixture of barium chloride, titanium(IV) chloride, H_2O, and diethylene glycol (DEG) at 220 °C for three hours. The hydrolysis of the titanium precursor under these reaction conditions produced irregularly shaped nanoparticles with sizes of approximately 3–10 nm, as shown in the transmission electron microscopy (TEM) image in Figure 1 a. When the TEM was operated in scanning mode (STEM), the composition and elemental distribution of the doped TiO_2 nanocrystals could be mapped through energy-dispersive X-ray spectroscopy (EDX) by displaying the integrated intensities of the Ti, Ba, and O signals as functions of the beam position. A comparison of the high-angle annular dark-field (HAADF) STEM image and the elemental maps of the Ba-doped TiO_2 nanocrystals shown in Figure 1 b confirms the even distribution of Ba in the TiO_2 nanocrystals.

The X-ray diffraction (XRD) pattern of the as-synthesized product is shown in Figure 1 c. All of the diffraction peaks are indexed to anatase TiO_2 with cell constants of $a =$ 3.7852 Å and $c = 9.5139$ Å (JCPDS No. 21-1272). No characteristic peaks of crystallographic Ba phase compounds could be found in the sample. The broadening of the diffraction peaks is consistent with the small size of the TiO_2 nanocrystals determined by TEM. Compared with the undoped TiO_2 nanocrystals, which exhibit a strong absorption from 250 to 375 nm with a long shoulder from 375 to 700 nm, a noticeable shift of approximately 16 nm to shorter wavelengths could be observed for the Ba-doped sample (Figure 1 d). The shift towards shorter absorption wavelengths is consistent with a prior observation by Venkatachalam and co-workers on the doping of TiO_2 with alkaline-earth metal ions.[7]

X-ray photoelectron spectroscopy (XPS) was further used to investigate the Ba doping in the TiO_2 nanocrystals. The

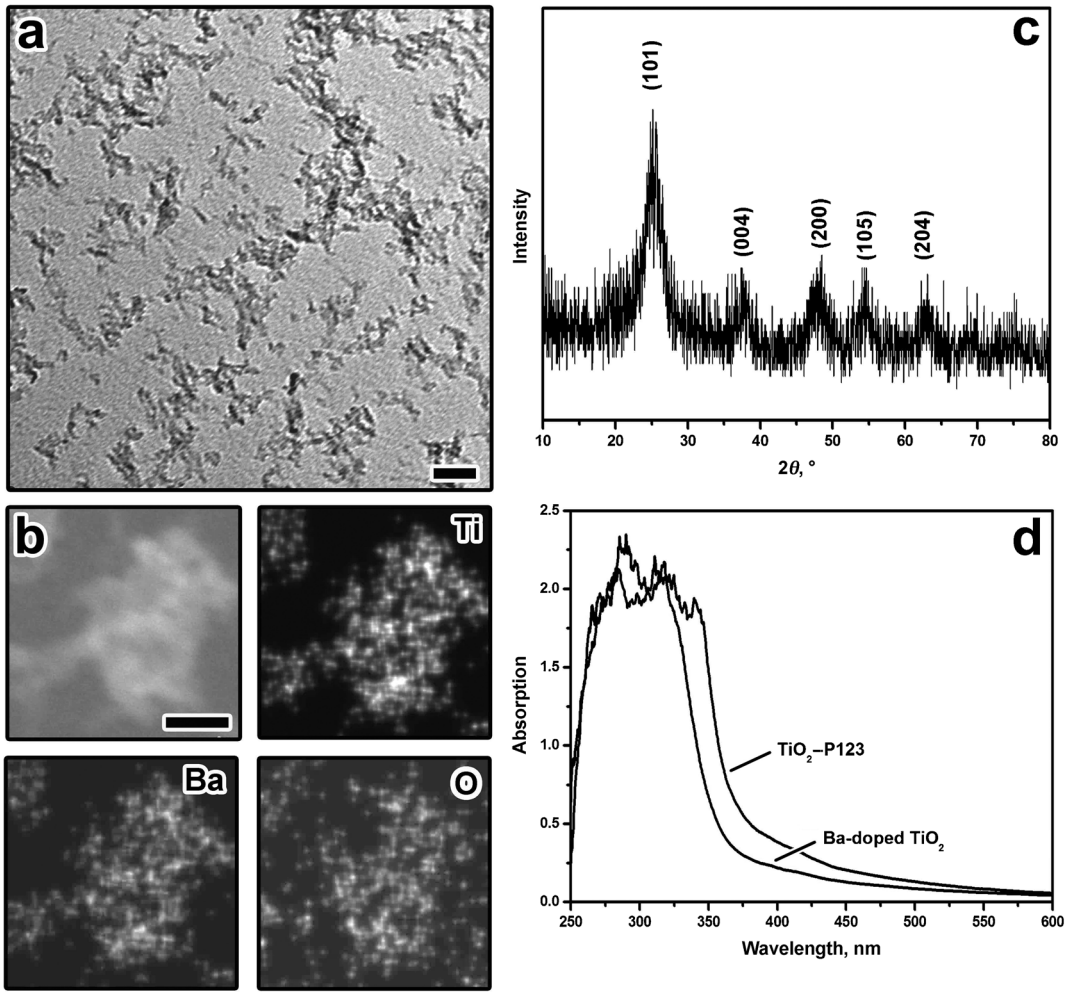

Figure 1. Characterization of as-synthesized Ba-doped TiO_2 nanocrystals: a) Typical bright-field TEM image. b) HAADF-STEM image and the corresponding elemental distribution of Ti, Ba, and O. c) XRD pattern. d) UV/Vis spectra. An area with nanocrystal aggregates was used for elemental mapping to obtain sufficient signal intensities. Scale bars: 20 nm (a), 10 nm (b).

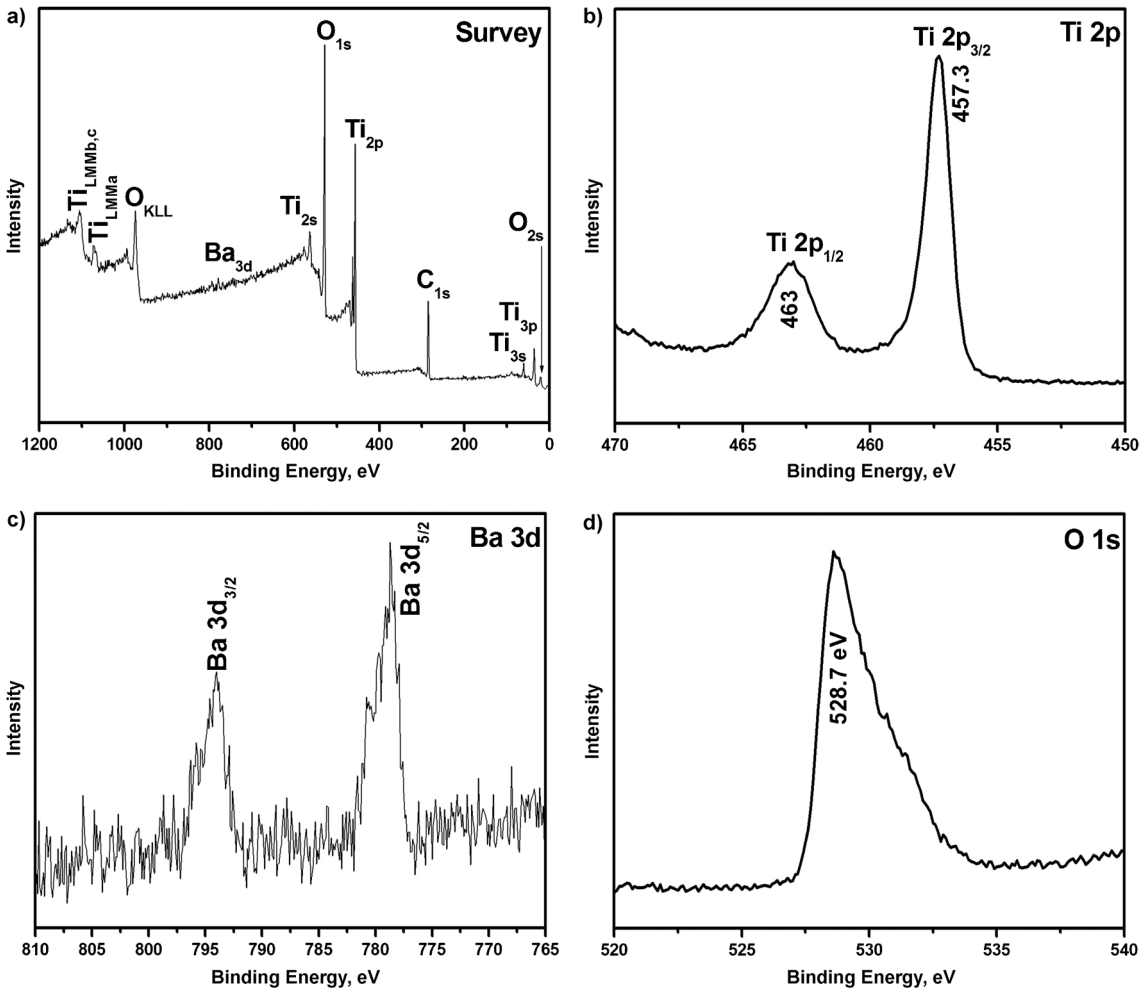

Figure 2. a) XPS survey spectrum of Ba-doped TiO_2 nanocrystals. b–d) High-resolution XPS spectra of the Ti 2p (b), Ba 3d (c), and O 1s (d) orbitals.

survey XPS spectrum in Figure 2a shows the Ti, O, and Ba signals. The existence of a C peak in the spectrum is probably due to residual solvent (DEG) or adsorbed CO_2. The binding energies of Ti $2p_{3/2}$ and Ti $2p_{1/2}$ are located at 457.3 and 463 eV, respectively (Figure 2b). Figure 2c shows the binding energies of Ba $3d_{5/2}$ and Ba $3d_{3/2}$ with peaks at 780 and 795 eV, clearly confirming the existence of barium in the TiO_2 nanocrystals.[8] No peak corresponding to Cl 2p could be detected in the Ba-doped TiO_2 nanocrystals. The atomic percentage of Ba relative to Ti was calculated from the XPS data to be approximately 1.2%. It has been reported that even such a small amount as 0.1% of a dopant in TiO_{2-x} thin films is equivalent to 5×10^{19} donors per cm^3.[8b,9] In such doped TiO_2 nanocrystals, the oxygen vacancies may act as effective SEDs promoting the charge separation that is required for redox-based color-switching systems.

X-ray absorption spectroscopy (XAS), with its high sensitivity to chemical and electronic structures, was used to identify the presence of oxygen vacancies in Ba-doped TiO_2 nanocrystals. The near-edge spectra (XANES) of standard TiO_2 powder display characteristic O K-edge peaks corresponding to two different energy ranges: 1) The region from 530 to 535 eV is associated with the transitions from the O 1s orbital to the hybridized orbitals of O 2p and Ti 3d. As the crystal field splits the 3d levels into t_{2g} and e_g, this gives rise to two contributions, which are labeled as A and B, respectively.[10] This splitting is very sensitive to the coordination number and the extent of the hybridization. 2) The range from 535 to 550 eV represents the transitions from the O 1s orbital to the O 2p antibonding orbital (peak C) and the O 2p/Ti 4sp band (peak D). Figure 3a shows the changes in the O K-edge spectra of Ba-doped TiO_2 nanocrystals under UV irradiation. The relative intensities of the t_{2g} and e_g peaks increased with increasing irradiation time, indicating an enhancement of the transitions from the O 1s orbital to the O 2p/Ti 3d hybridized orbitals.[6a] We assume that UV irradiation promotes the oxidation of TiO_2 nanocrystals and reduces the amount of oxygen vacancies resulting from the Ba doping.[11] In other words, the oxygen vacancies in the Ba-doped TiO_2 may scavenge the holes produced under UV irradiation, therefore enhancing the transitions from the O 1s orbital to the hybridized orbital between O 2p and Ti 3d.

The Ti L-edge XANES spectrum gives direct information on the unoccupied d orbitals of the Ti ions where electron

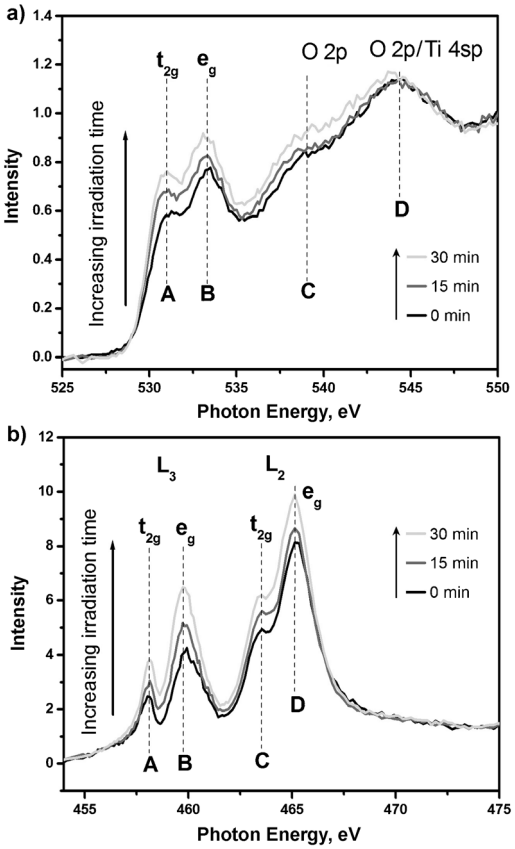

Figure 3. a, b) XANES spectra of the O K-edge (a) and the Ti L-edge (b) of Ba-doped TiO_2 nanocrystals with increasing irradiation time under vacuum.

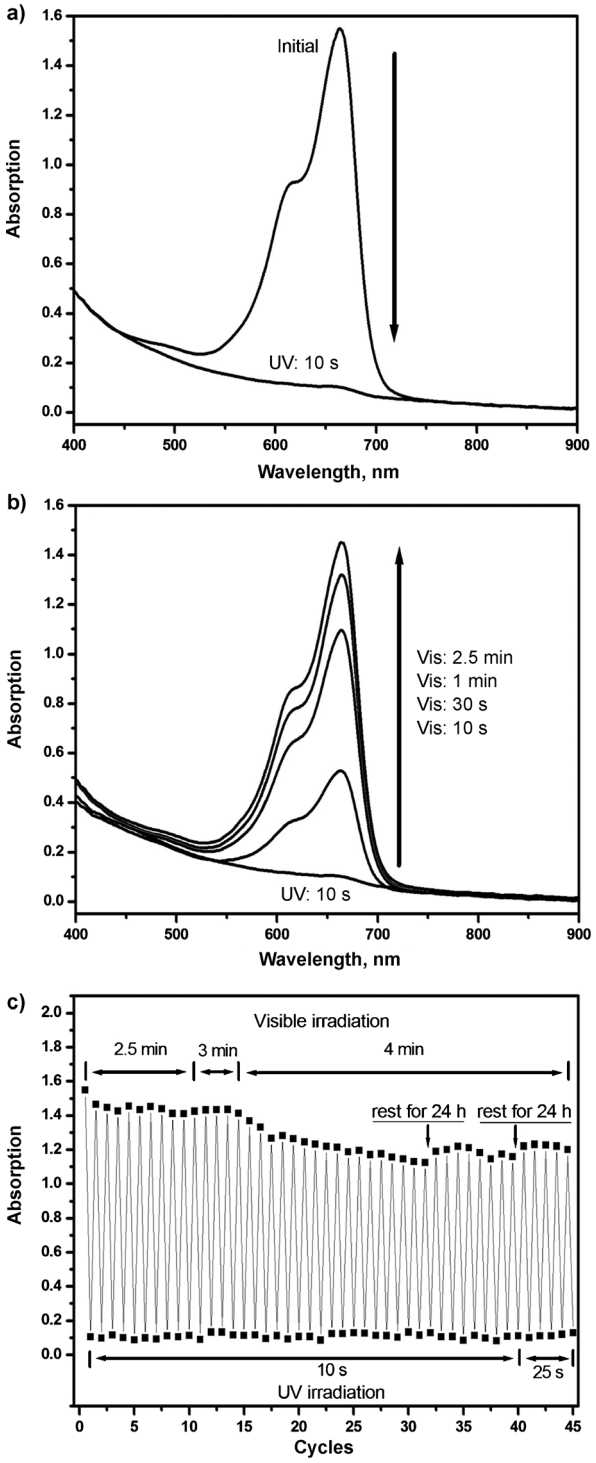

Figure 4. Light-responsive color switching of the Ba-doped TiO_2 nanocrystals/MB/water system upon UV and visible-light irradiation. a) UV/Vis spectra showing the decoloration process under UV irradiation during the first cycle of color switching. b) UV/Vis spectra showing the recoloration process under visible-light irradiation in the first cycle of color switching. c) The absorption intensity at approximately 660 nm of the mixture under alternating UV and visible-light irradiation for 45 cycles.

transfer occurs. The Ti L-edge XANES spectrum consists of two sets of peaks, L_3 and L_2, which correspond to electronic transitions from the $2p_{3/2}$ and $2p_{1/2}$ orbitals to a 3d excited state of the Ti atoms, respectively.[12] Owing to the splitting of the 3d orbitals into t_{2g} and e_g states, each L peak consists of two contributions. Figure 3b reveals that both the Ti L_3 and L_2 edges represent t_{2g}-like and e_g-like orbitals. Similar to the O K-edge spectrum, the relative intensities of the t_{2g} and e_g peaks increase with increasing irradiation time, further indicating the elimination of oxygen vacancies during UV irradiation.[13] Both the O K-edge and Ti L-edge XANES spectra clearly corroborate the existence of oxygen vacancies in the original Ba-doped TiO_2 nanocrystals, which are consumed gradually by scavenging holes during UV irradiation.

The Ba-doped TiO_2 nanocrystals/MB/water system exhibits an unprecedented cyclability and a high rate of photoreversible color switching. Upon UV irradiation, the blue color of the mixture disappears in a short period of ten seconds (Figure 4a). Although no P123 is present, the oxygen vacancies in the Ba-doped TiO_2 nanocrystals can act as SEDs to directly capture the photogenerated holes, enabling the rapid reduction of MB to LMB by the remaining photogenerated electrons. As a result, the color of the system switched from blue to colorless. The absorption spectra of the same system gradually reversed direction, and the original spectra were fully recovered within approximately 2.5 minutes upon visible-light irradiation (Figure 4b), which

is six times faster than for the P123-capped TiO_2 nanocrystals that we previously described.[3] The enhanced recoloration rate is believed to be related to the shift of the absorption wavelength of Ba-doped TiO_2 nanocrystals to a shorter wavelength. As previously revealed, the recoloration process operates dominantly by the self-catalyzed oxidation of LMB, which is however countered by a competing reverse reduction reaction of MB by photoelectrons generated from TiO_2 nanocrystals by visible-light irradiation owing to the considerable absorption of TiO_2 in the visible region. With Ba-doped TiO_2 nanocrystals, the shift in the absorption to a shorter wavelength minimizes the reverse reduction reaction, leading to a faster recoloration process. When the Ba-doped TiO_2 nanocrystals/MB/water system was initially purged with nitrogen to remove dissolved oxygen and then exposed to visible-light irradiation, the intensity of the MB absorption did not change even after 20 minutes (see the Supporting Information, Figure S1), further confirming that the Ba-doped TiO_2 nanocrystals could not be excited by visible-light irradiation to reduce MB. The recoloration process of the Ba-doped TiO_2 nanocrystals/MB/water system upon visible-light irradiation was also studied using different bandpass filters (FWHM: 25 nm), the corresponding UV/Vis spectra are shown in Figure S2. As previously described for TiO_2 nanocrystals, the use of light sources with bandpass filters at various different wavelengths (370–700 nm) can enhance the recoloration rate of MB from LMB, corroborating the previously proposed mechanism of light-catalyzed oxidation of LMB by oxygen, although the reactions that take place under UV and visible-light irradiation are completely different.[3]

In our previous color-switching system, the photogenerated holes were captured by P123 molecules bound on the surface of the nanocrystals, which were depleted by photogenerated holes under UV irradiation after several cycles already. The Ba-doped TiO_2 nanocrystals, which utilize oxygen vacancies as SEDs, allow reversible switching for significantly greater number of cycles. The peak intensities of the MB absorption peak at approximately 660 nm after UV and visible-light irradiation for multiple cycles are plotted in Figure 4c, demonstrating the unprecedented high reversibility. We first repeated the switching process continuously for 31 cycles, and the system displayed full reversibility in spite of a small decrease in the absorption intensity of the blue state after 15 cycles. After resting the system in air for approximately 24 hours, the absorption intensity of the blue state had slightly recovered. The switching process was then repeated continuously for another eight cycles, in which the absorption intensity of the blue state started to decrease after four cycles. When the sample was rested for another 24 hours, the intensity was recovered again and started to fall off after another four continuous switching cycles. More interestingly, when the sample was rested in air for one year, the absorption intensity of the system fully recovered to its original value, and the reversible color-switching process could be repeated again for several cycles (Figure S3).

The recovery of the absorption intensity of the blue state after resting is believed to be due to the continued oxidation of residual LMB. After 15 cycles of continuous color switching, the catalytic performance of the TiO_2 nanocrystals started to decay owing to the gradual consumption of the oxygen vacancies. This decay first affected their efficiency in catalyzing the oxidation of LMB in the recoloration step so that much longer times were needed to recover MB. Even after extending the visible-light irradiation time from the original 2.5 minutes to 3 minutes and eventually 4 minutes, a small fraction of LMB molecules still remained, leading to the overall reduction in absorption intensity of the blue state. After resting the system in air for 24 hours, the remaining LMB molecules were partially oxidized, contributing to the slight increase in the absorption intensity of MB.

The current photoreversible color-switching system may find a wide range of practical applications, especially as a rewritable paper. Therefore, we now describe the fabrication of a solid rewritable paper by drop-casting a mixture of Ba-doped TiO_2 nanocrystals, MB, hydroxyethyl cellulose (HEC), EG, and H_2O on a glass substrate followed by drying the film at 60 °C and further annealing at 120 °C (Figure 5 and Figure S4). Letters can be printed successfully on the rewritable paper by UV irradiation through a photomask, which was pre-made by ink-jet printing on a transparent plastic film. After UV irradiation for approximately one

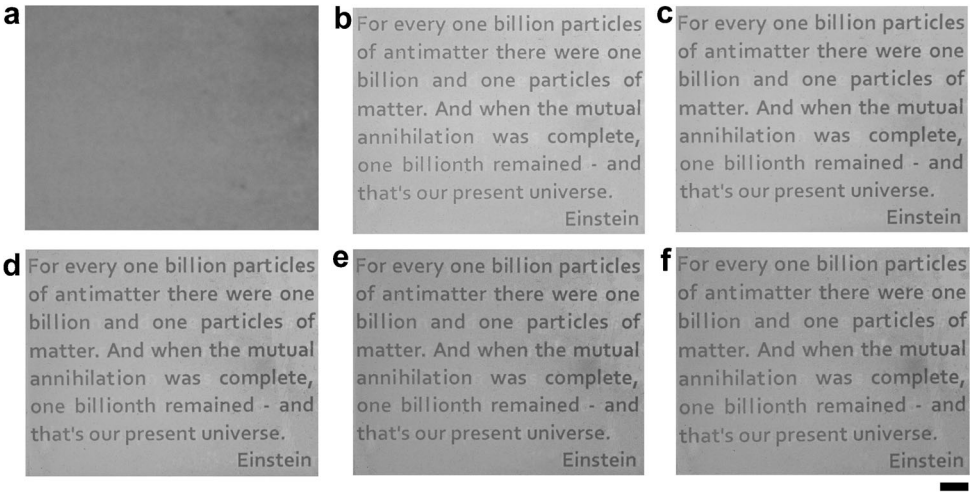

Figure 5. Photographs of a rewritable paper obtained by casting the Ba-doped TiO_2/MB/HEC mixture onto a glass substrate. a) Original film after drying. b–f) Letters were printed on the film by UV irradiation through a photomask; the film was then kept under ambient conditions for 10 minutes (b), one day (c), two days (d), three days (e), and four days (f). Scale bar: 5 mm. The photomask was produced by ink-jet printing on a transparent plastic.

minute, the exposed regions turned to colorless while the unexposed regions retained the blue color, replicating letters from the photomask to the film (Figure 5b). The blue letters of font size 12 could be easily printed with very good resolution, and they remained highly legible for at least four days under ambient conditions (Figure 5c–f), which is sufficiently long for most temporary reading purposes. In fact, the printed letters remained legible for seven days although the background gradually turned into light blue owing to the graduate oxidation of LMB under ambient conditions (Figure S5). The oxidation of LMB in the film by ambient oxygen was significantly delayed by HEC, which could stabilize LMB through hydrogen bonding.[4,6b] On the other hand, the prints can be erased completely by heating the rewritable paper in air at 120 °C for approximately 30 minutes. During heating, the re-oxidation of LMB was enhanced so that the decoloration process can be completed within a considerably shorter period of time. The recovered film can be used again for printing letters/patterns by UV irradiation through a photomask, still with high contrast and resolution (Figure S6). Considering the significantly improved reversibility and repeatability compared with our previously described P123/TiO_2-based system, we believe that the new rewritable paper represents a big step towards practical applications. To demonstrate the high printing resolution, we have exposed the film to UV light through a chrome photomask with microscale patterns. As shown in Figure S7, various patterns with sizes from 550 to 90 μm could be replicated on the film with sharp edges, clearly showing the potential for achieving high resolution beyond the limit of the naked eye.

In summary, we have described the colloidal synthesis of Ba-doped TiO_2 nanocrystals, which can be used for the highly reversible light-responsive color switching of redox dyes at significantly enhanced rates and with improved cycling performance. Oxygen vacancies resulting from the Ba doping can effectively scavenge the holes photogenerated in TiO_2 nanocrystals under UV irradiation and therefore enable color switching without relying on external SEDs, thus greatly increasing the number of switching cycles. Ba doping also shifts the absorption of the TiO_2 nanocrystals to a shorter wavelength, effectively repressing the partial reduction of MB to LMB under visible-light irradiation and therefore leading to a higher recoloration rate. Such a mixture can also be casted into a solid film on which letters and patters can be printed using UV light, which can then be erased again by heating; this printing process can be repeated for many cycles and does not require additional inks.

Received: October 23, 2014

Keywords: doping · nanocrystals · oxygen vacancies · photocatalysis · titania

[1] a) K. Li, Y. Xiang, X. Y. Wang, J. Li, R. R. Hu, A. J. Tong, B. Z. Tang, *J. Am. Chem. Soc.* **2014**, *136*, 1643 – 1649; b) J. X. Bu, K. Watanabe, H. Hayasaka, K. Akagi, *Nat. Commun.* **2014**, *5*, 2799; c) L. García-Fernández, C. Herbivo, V. S. Arranz, D. Warther, L. Donato, A. Specht, A. del Campo, *Adv. Mater.* **2014**, *26*, 5012 – 5017; d) Y. L. Rao, C. Horl, H. Braunschweig, S. N. Wang, *Angew. Chem. Int. Ed.* **2014**, *53*, 9086 – 9089; *Angew. Chem.* **2014**, *126*, 9232 – 9236; e) Y. Wu, Y. S. Xie, Q. Zhang, H. Tian, W. H. Zhu, A. D. Q. Li, *Angew. Chem. Int. Ed.* **2014**, *53*, 2090 – 2094; *Angew. Chem.* **2014**, *126*, 2122 – 2126.

[2] R. A. Evans, T. L. Hanley, M. A. Skidmore, T. P. Davis, G. K. Such, L. H. Yee, G. E. Ball, D. A. Lewis, *Nat. Mater.* **2005**, *4*, 249 – 253.

[3] W. Wang, M. Ye, L. He, Y. Yin, *Nano Lett.* **2014**, *14*, 1681 – 1686.

[4] W. Wang, N. Xie, L. He, Y. Yin, *Nat. Commun.* **2014**, *5*, 5779.

[5] a) K. Lai, W. Wei, Y. Zhu, M. Guo, Y. Dai, B. Huang, *J. Solid State Chem.* **2012**, *187*, 103 – 108; b) S. A. Bilmes, P. Mandelbaum, F. Alvarez, N. M. Victoria, *J. Phys. Chem. B* **2000**, *104*, 9851 – 9858; c) I. Nakamura, N. Negishi, S. Kutsuna, T. Ihara, S. Sugihara, K. Takeuchi, *J. Mol. Catal. A* **2000**, *161*, 205 – 212; d) G. Pacchioni, *ChemPhysChem* **2003**, *4*, 1041 – 1047; e) M. K. Nowotny, L. R. Sheppard, T. Bak, J. Nowotny, *J. Phys. Chem. C* **2008**, *112*, 5275 – 5300.

[6] a) T. Okumura, T. Fukutsuka, A. Yanagihara, Y. Orikasa, H. Arai, Z. Ogumi, Y. Uchimoto, *J. Mater. Chem.* **2011**, *21*, 15369 – 15377; b) B. S. Liu, L. P. Wen, K. Nakata, X. J. Zhao, S. H. Liu, T. Ochiai, T. Murakami, A. Fujishima, *Chem. Eur. J.* **2012**, *18*, 12705 – 12711; c) X. Pan, M.-Q. Yang, X. Fu, N. Zhang, Y.-J. Xu, *Nanoscale* **2013**, *5*, 3601 – 3614.

[7] N. Venkatachalam, M. Palanichamy, B. Arabindoo, V. Murugesan, *Catal. Commun.* **2007**, *8*, 1088 – 1093.

[8] a) K. Zhang, Z. H. Zhou, L. J. Guo, *Int. J. Hydrogen Energy* **2011**, *36*, 9469 – 9478; b) C. C. Hu, M. S. Lin, T. Y. Wu, F. Adriyanto, P. W. Sze, C. L. Wu, Y. H. Wang in *Physics and Technology of High-K Materials 9*, *Vol. 41* (Eds.: S. Kar, S. VanElshocht, K. Kita, M. Houssa, D. Misra), The Electrochemical Society, Pennington, New Jersey, USA, **2011**, pp. 439 – 444.

[9] N. M. M. Vujisic, I. Fetahovic, K. Stankovic, P. Osmokrovic, *Sci. Publ. State Univ. Novi Pazar* **2012**, *4*, 75 – 82.

[10] S. J. Stewart, M. Fernandez-Garcia, C. Belver, B. S. Mun, F. G. Requejo, *J. Phys. Chem. B* **2006**, *110*, 16482 – 16486.

[11] S. C. Chen, K. Y. Sung, W. Y. Tzeng, K. H. Wu, J. Y. Juang, T. M. Uen, C. W. Luo, J. Y. Lin, T. Kobayashi, H. C. Kuo, *J. Phys. D* **2013**, *46*, 075002.

[12] A. Ohtomo, D. A. Muller, J. L. Grazul, H. Y. Hwang, *Nature* **2002**, *419*, 378 – 380.

[13] D. A. Muller, N. Nakagawa, A. Ohtomo, J. L. Grazul, H. Y. Hwang, *Nature* **2004**, *430*, 657 – 661.

